Supplement

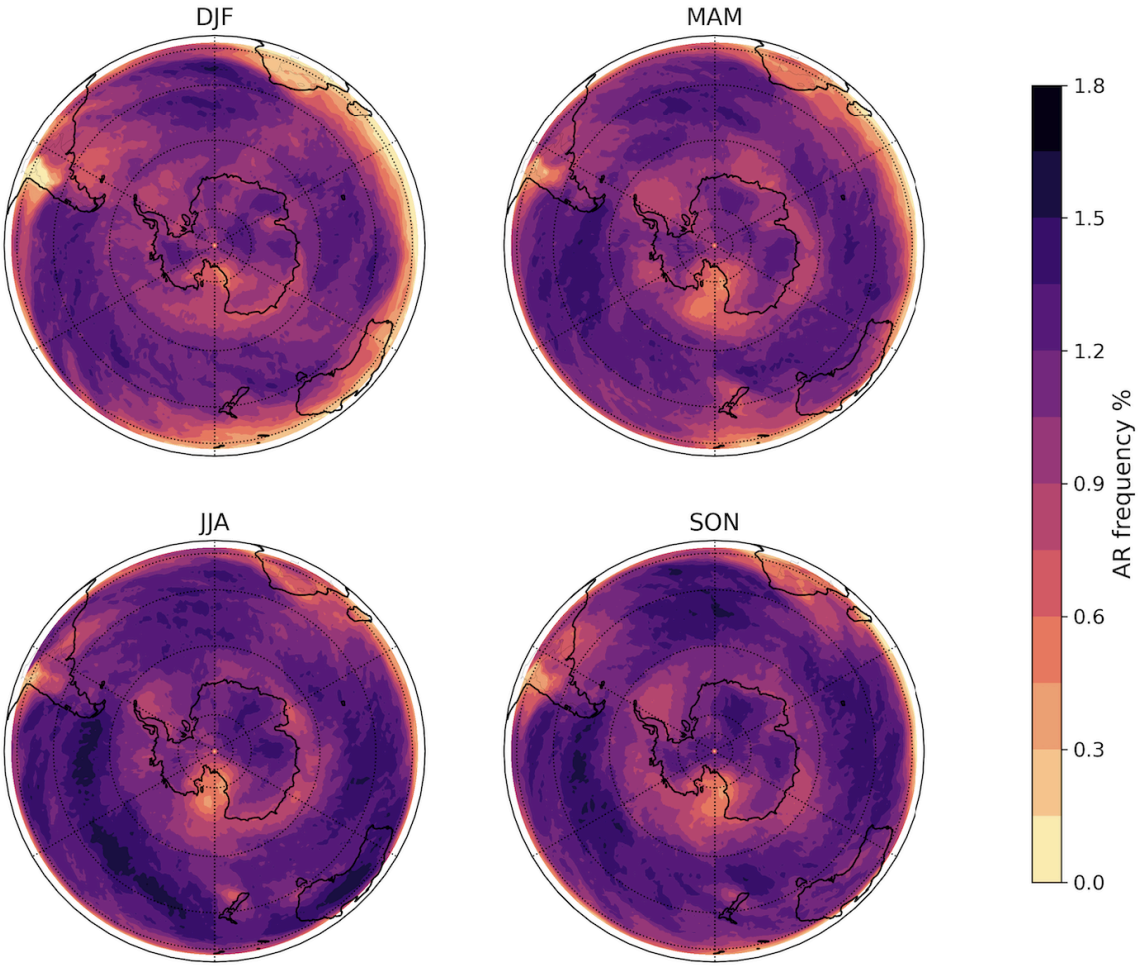

Fig. S1. Seasonal frequency of DARK ARs for all four austral seasons (DJF, MAM, JJA, SON).

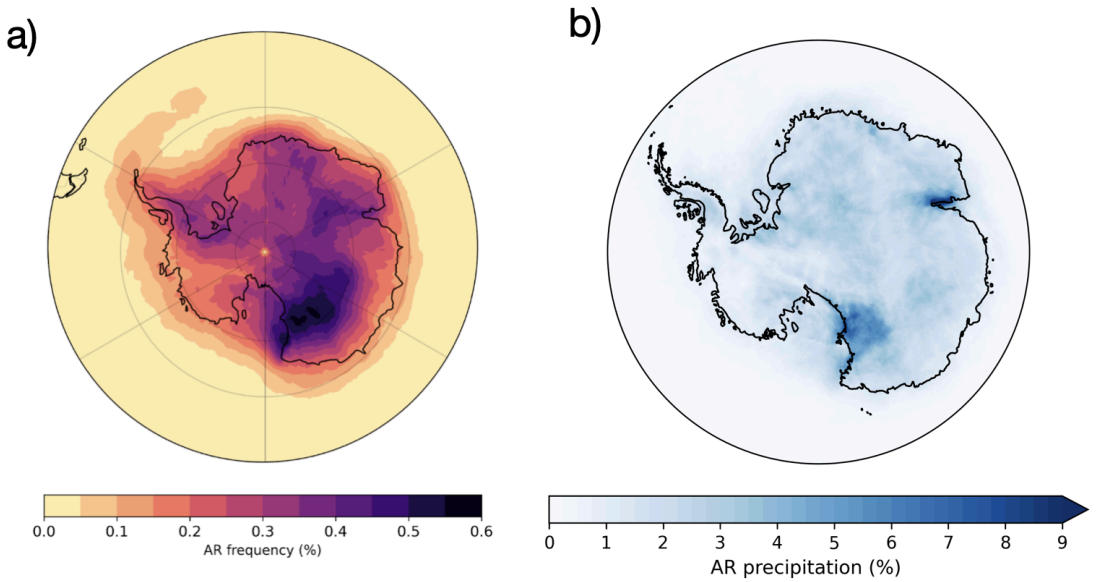

Fig. S2. (a) Frequency of DARK AR-children (similar to **Fig. 2**). (b) Share of total precipitation attributed to DARK AR-children (similar to **Fig. 4**).

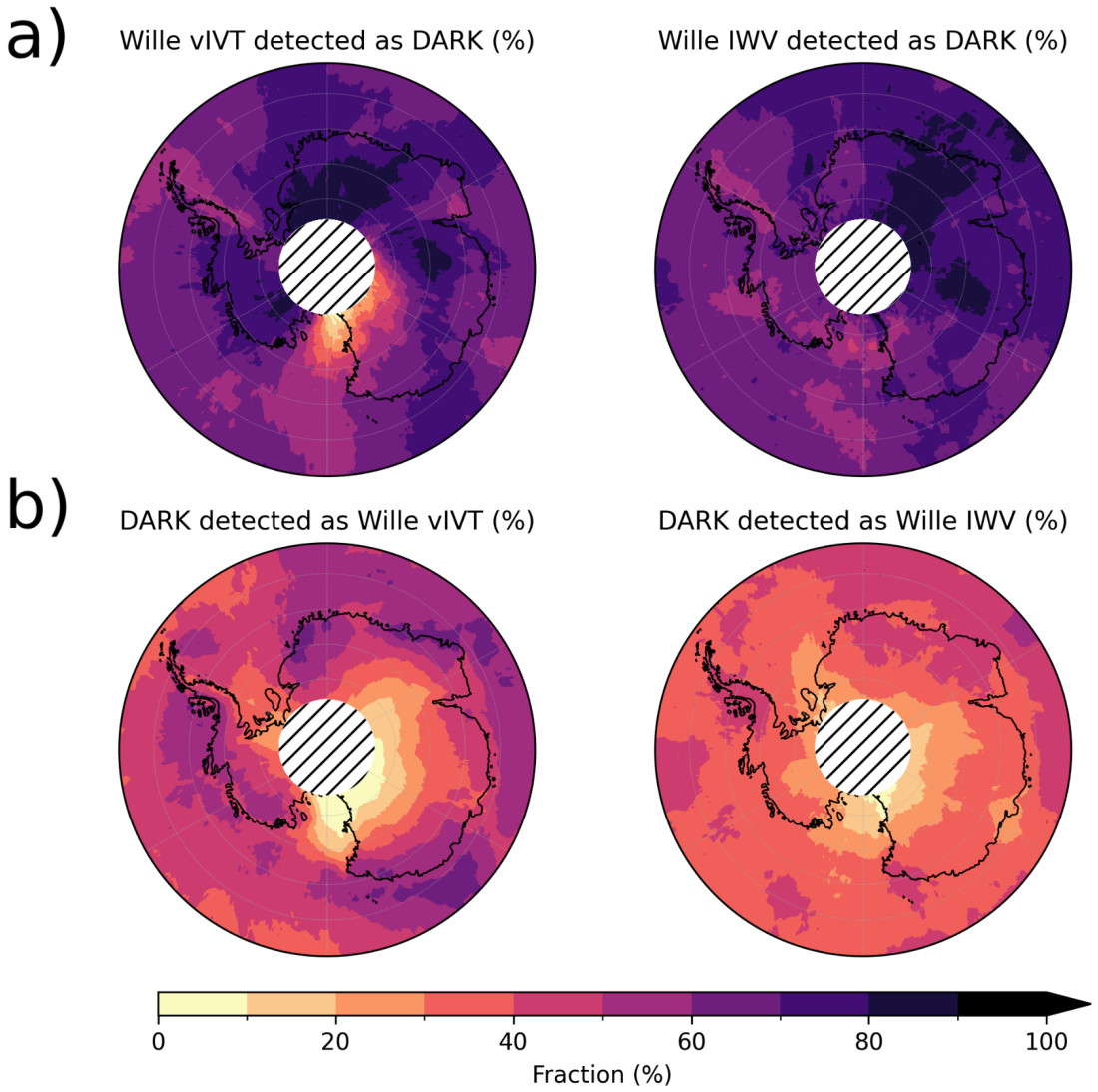

Fig. S3. Co-detection fractions between the DARK and Wille vIVT (left) and Wille IWV (right) catalogues. Panels show, for each grid point, the percentage of detections in one catalogue that have a corresponding detection in the other within a ± 2° latitude × ± 5° longitude neighbourhood. (a) Wille detections identified as DARK. (b) DARK detections identified as Wille. The area poleward of 83° S is masked (hatched) to avoid edge effects introduced by the ± 2° latitude neighbourhood near the pole.

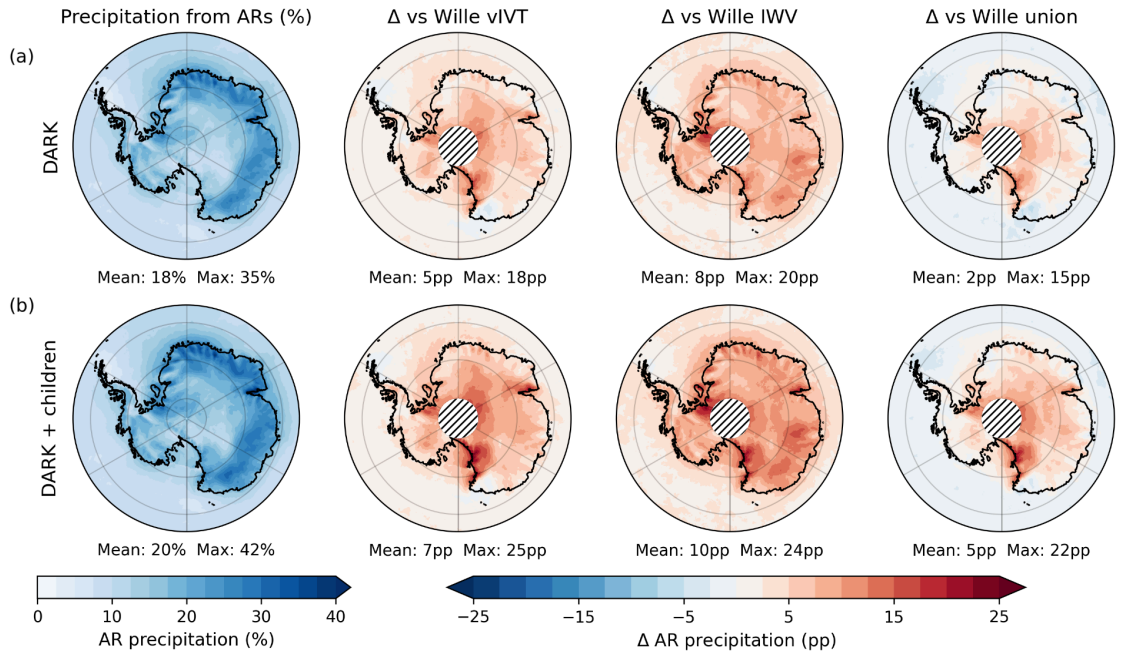

Fig. S4. Same as **Fig. 3**, with an additional column showing the difference in AR-attributed precipitation relative to the combined Wille vIVT + IWV ("Wille union") scheme. Antarctic land-only mean and maximum values are reported below each panel. Hatched white areas south of 85° S mark regions excluded from the Wille schemes.

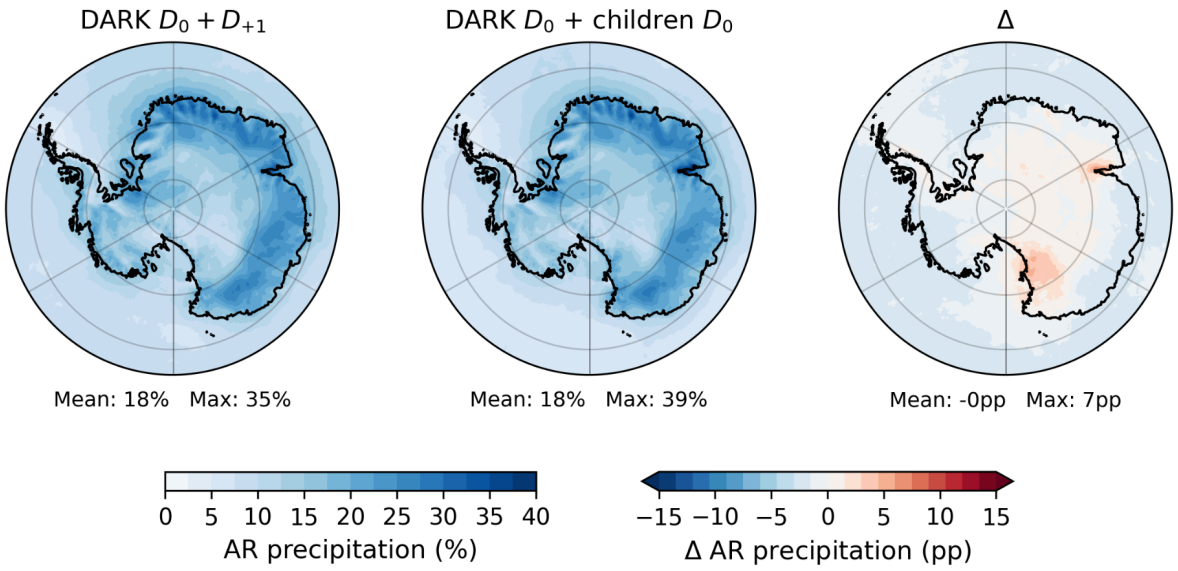

Fig. S5. Share of total precipitation attributed to (left) DARK ARs, including precipitation occurring on the day of landfall (D_0) and the following day (D_{+1}); (middle) DARK ARs and their children considering only the day of landfall (D_0); and (right) their difference (left – middle).

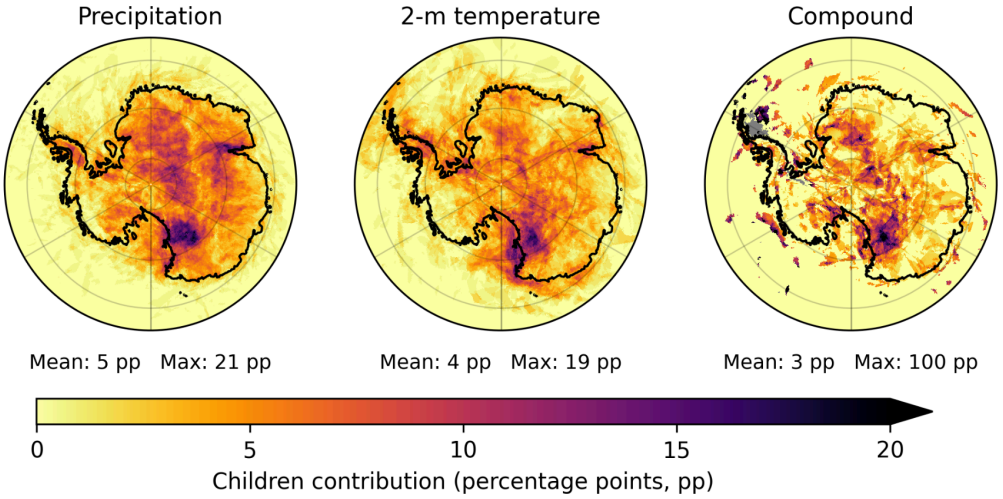

Fig. S6. Contribution of AR children to the fraction of 99th-percentile anomaly days associated with DARK ARs and their children (displayed in Fig. 5b, d and Fig. 6d).

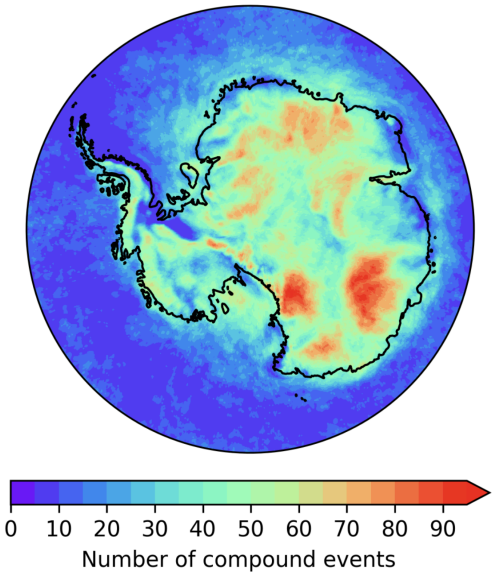

Fig. S7. Number of compound precipitation–temperature extreme events (Sect. 2.4) across Antarctica.